Theory of the spin dependence of the inelastic mean free path of electrons in ferromagnetic metals: A model study

Jisang Hong and D. L. Mills
Department of Physics and Astronomy, University of California, Irvine, California 92697
(Received 11 January 1999)

We explore the spin dependence of the inelastic mean free path of an excited electron in a model ferromagnetic metal. The excited electron is assumed to reside in a plane-wave state, while the metal electrons are modeled within the framework of a one-band Hubbard model. We consider scattering by both Stoner excitations and by spin waves, and outline their relative importance in various energy ranges. In addition, we explore the dependence of the inelastic mean free path on the number of holes in the spin-polarized energy bands of the substrate. [S0163-1829(99)11821-6]

I. INTRODUCTION

Various spin-polarized electron spectroscopies are employed to probe the surfaces of magnetic materials and also ultrathin films. Examples are provided by photoemission studies in which the spin of the photoelectron is detected, scattering experiments such as spin-polarized low-energy electron diffraction (SPLEED), and the spin-polarized version of electron energy loss spectroscopy (SPEELS).[1] If these and other related spectroscopies employ electrons with energy in the range from 1 to 100 eV, they display great surface sensitivity by virtue of the fact that the electron mean free path is only two or three lattice constants, in most materials of interest. The strong inelastic scattering of the probe electron from particle-hole excitations and collective excitations (plasmons, for example) leads to such short mean free paths.

In a ferromagnetic metal, quite clearly the probe electron mean free path will be spin dependent, and different for the cases where its spin is parallel or antiparallel to the substrate magnetization. A quantitative understanding of the spin dependence of the inelastic mean free path is essential to an interpretation of the information obtained from polarized probes. For example, one may wish to use a spin-polarized electron photoemitted from the $3d$ bands of ferromagnetic metal as a means of the presence of enhanced magnetic moments in the surface or the temperature variation of the near-surface magnetization. The interpretation of such data is affected sensitively by a difference between the mean free path of spin-up and spin-down photoelectrons, if this is substantial.

Various experiments have explored the question of the spin-dependent mean free path. An elegant example is provided by the work of Pappas *et al.*[2] These authors deposited an ultrathin ferromagnetic Fe film on a Cu(110) surface. Electrons were excited from the Cu $3d$ bands with sufficient energy to emerge above the vacuum level after passing through the Fe film. A substantial spin asymmetry in the photocurrent was detected. It was argued[2] that the spin asymmetry has its origin in the spin dependence of the inelastic photoelectron mean free path, However, subsequent theoretical calculations[3] showed that spin-dependent *elastic* scattering of the photoelectron accounted nicely for both the magnitude and energy variation of the measured asymmetry. This along with the fact that a very extensive set of SPLEED data (taken with beam electrons whose kinetic energy is much larger that those sampled in Ref. 2) on Fe(110) may be accounted for in a remarkably quantitative manner without the need to incorporate spin asymmetry in the beam penetration depth[4] suggests that the spin asymmetry in the inelastic mean free path of excited electrons may be more modest than that assumed by some authors. Clearly theoretical studies of this question are highly relevant. We hasten to add that in a very beautiful experiment, clear and unambiguous measurements of spin-dependent quasiparticle lifetimes have been reported, for excited electrons roughly 1 eV above the Fermi energy of ferromagnetic Co.[5]

In this paper, we explore the spin dependence of the electron mean free path in a simple model we believe sufficiently complete to allow conclusions to be drawn regarding a number of issues. The virtue of the model is its simplicity; within it we can readily derive expressions whose structure may be explored by analytic means. In the numerical studies below, we can easily vary parameters to see trends in the spin dependence as we vary the number of holes in the substrate energy bands, the magnetic moment of the substrate, and so on. It is our intention to carry out fully quantitative studies of the spin dependence of the electron mean free path, for fully realistic pictures of the transition metal ferromagnets, in the near future.

The excited electron is assumed here to reside in a plane-wave state, while the electrons in the substrate are described within the framework of the one-band Hubbard model. Mean field theory provides us with a model of a ferromagnetic ground state, and we use the random phase approximation to describe the spin excitations (spin waves, Stoner excitations) sampled by the excited electron. Our analysis includes the influence of spin waves on the mean free path; we find these dominate at low quasiparticle energies such as those sampled in Ref. 5.

The outline of this paper is as follows. In Sec. II, we introduce the model and the formalism used to generate our expression for the spin-dependent contribution to the inelastic mean-free path. Section III examines a special limiting case, the contributions from scatterings produced by the

emission or absorption of long-wavelength spin waves. Section IV presents numerical studies, and final remarks are found in Sec. V.

II. MODEL AND THEORETICAL CONSIDERATIONS

As mentioned in Sec. I, we model the substrate electrons within the framework of the one-band Hubbard model. The excited electron whose mean free path is the subject of our interest will be supposed to be in a plane-wave state, a picture appropriate for a simple model of an electron with energy above the vacuum level. We ignore multiple-scattering events experienced by such electrons that are, of course, important in the analysis of data such as photoemission data. We generate expressions for the spin-dependent mean free path by exploring the relevant contributions to the self-energy of such electrons. We note that in full multiple-scattering theories, self-energies calculated in this manner provide the basis for modeling the imaginary part of the inner potential, in full treatments of multiple scattering.[6] Thus, our analysis can provide input for such full calculations when applied to ferromagnetic materials. We shall also let the energy of the excited electron approach the Fermi energy. We then view our model as providing a description of electrons associated with the *sp* bands of transition metals. In this energy regime, we invoke the two-band picture of transition metals, viewed as materials with magnetic properties derived from tight-binding $3d$ bands, and transport by electrons of *sp* character. It is then the mean free path of an *sp* electron we are considering. The numerical calculations, interpreted as just described, may be used to explore trends. It is our intention to carry out calculations which employ a realistic structure of the ferromagnetic transition metals in the near future, as mentioned above. The analysis here serves as a starting point for such studies.

The Hamiltonian is then

$$H=\sum_{i,j} t_{i,j}c^{\dagger}_{i\sigma}c_{j\sigma}+U_0\sum_i n_{i\uparrow}n_{i\downarrow}+V_{ex}+H_e\,. \qquad (1)$$

The first two terms describe the band electrons. We use a bcc lattice, and nearest-neighbor hopping only. The term H_e describes the excited electron and V_{ex} the exchange scattering of it off the band electrons.

We shall explore the basic exchange process illustrated schematically in Fig. 1(a), and described by the diagram in Fig. 1(b). In Fig. 1(a), we have an excited spin-down electron propagating in the material, illustrated by a solid circle. This makes the transition to an unoccupied hole state in the minority spin band of the substrate and via the Coulomb interaction excites an electron from the majority spin band to the final state. We thus have an exchange-induced spin flip of the excited electron, accompanied by creation of a spin-triplet particle-hole pair in the substrate energy bands. The spin-triplet particle-hole pair is referred to as a Stoner excitation.

We discuss the form of the matrix element which controls the exchange scattering event depicted in Fig. 1. It was found that in a recent theoretical analysis of the contribution of the spin-flip processes to energy losses experienced by an electron propagating in ferromagnetic Fe,[7] the ratio of losses via spin-wave excitation to those from coupling to Stoner excitations is sensitive to the structure of the exchange matrix element. Thus, we wish to use a realistic form for this in the analysis here, since we wish to assess the relative importance of the two mechanisms to the inelastic mean free path. For the process illustrated in Fig. 1(b), we consider

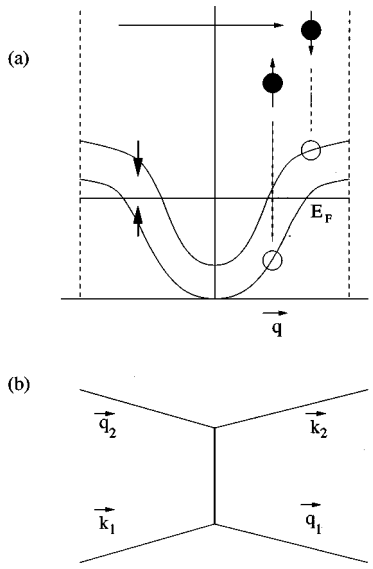

FIG. 1. (a) An illustration of the basic exchange process explored in this paper. An excited electron with spin down drops into an empty state in the minority spin band, while it excites a majority spin electron to an excited state via the Coulomb interaction. (b) A diagram of the process illustrated schematically in (a). Here $\vec{k}_1$ and $\vec{k}_2$ are the wave vectors of the excited electron in the initial and final states, while $\vec{q}_1$ and $\vec{q}_2$ are those for the band electron.

$$V_{ex}(\vec{k}_1,\vec{q}_2;\vec{q}_1,\vec{k}_2) = \int d^3x d^3y\, \psi^*_{\vec{q}_1}(\vec{x})\psi^*_{\vec{k}_2}(\vec{y})V(\vec{x}-\vec{y})\psi_{\vec{q}_2}(\vec{x})\psi_{\vec{k}_1}(\vec{y}). \qquad (2)$$

Then, if V is the volume of the crystal and N the number of unit cell within it, we have for the wave function of the excited electron

$$\psi_{\vec{k}}(\vec{x})=\frac{1}{\sqrt{V}}e^{i\vec{k}\cdot\vec{x}} \qquad (3)$$

and that in the substrate energy bands

$$\psi_{\vec{q}}(\vec{x})=\frac{1}{\sqrt{N}}\sum_{\vec{l}}\varphi(\vec{x}-\vec{l})e^{i\vec{q}\cdot\vec{x}}, \qquad (4)$$

where $\varphi(\vec{x}-\vec{l})$ is the localized orbital associated with site $\vec{l}$. We write the electron-electron interaction in the form

$$V(\vec{x}-\vec{y})=\sum_{\vec{p}} v(\vec{p})e^{i\vec{p}\cdot(\vec{x}-\vec{y})}. \qquad (5)$$

Then, following Ref. 7, we find

$$V_{ex}(\vec{k}_1,\vec{q}_2;\vec{q}_1,\vec{k}_2)=\frac{1}{V_c}\sum_{\vec{G}}\delta_{\vec{k}_1+\vec{q}_2;\vec{k}_2+\vec{q}_1-\vec{G}}\times\sum_{\vec{G}'}v(\vec{k}_1-\vec{q}_1+\vec{G}')\times f(\vec{k}_1-\vec{q}_1+\vec{G}'-\vec{k}_2)f(\vec{q}_1-\vec{G}'). \quad (6)$$

Here V_c is the volume of the unit cell, $f(\vec{q})$ the Fourier transform of the local orbital, and $\vec{G}$ is a reciprocal lattice vector. We have

$$f(\vec{q})=\int d^3x\varphi(\vec{x})e^{i\vec{q}\cdot\vec{x}}. \quad (7)$$

As in Ref. 7, we take $v(\vec{p})$ to the Fourier transform of the bare Coulomb interaction. We shall encounter predominantly scattering processes in which the wave vector transfer and energy loss are sufficiently large that screening may be viewed as unimportant. Thus, we choose the bare Coulomb interaction for $V(\vec{r}-\vec{r}')$. This is discussed further in Ref. 7. For $\varphi(\rho)$, we shall use the radial wave function for Fe employed by Pickett and co-workers.[8] This has the form

$$\varphi(\rho)=N_0\sum_{j=1}^{8}\alpha_jA_je^{-g_j\rho^2}, \quad (8)$$

where N_0 is a normalization constant, $\alpha_j=g_j^{7/4}/\sqrt{3}\pi^{3/4}$, and A_j is found by fitting the radial wave function to those determined from *ab initio* calculations.

With the form of the exchange matrix element in hand, we turn next to the analysis of the spin-dependent contribution to the mean free path. We shall proceed by examining the self-energy of the excited electron, with attention to those contributions which describe its spin flip scattering off spin excitations. In the ferromagnetic state, this scattering rate will differ for the two spin orientations of the beam electron. The issue is to explore the Green's function $G_\sigma(\vec{k},E)$ which describes propagation of the electron. This is written

$$G_\sigma(\vec{k},E)=\frac{1}{E-\epsilon_\sigma(\vec{k})-\Sigma_\sigma(\vec{k},E)}, \quad (9)$$

where $\epsilon_\sigma(\vec{k})=\hbar^2k^2/2m+V_\sigma$, and V_σ is a possibly complex spin-dependent, spatially averaged inner potential. We shall see below this inner potential enters importantly. Here $\Sigma_\sigma(\vec{k},E)$ is the proper self-energy of the excited electron.

Our interest, once again, is in those contributions to the self-energy which describe spin-flip processes. Within the language of finite-temperature many-body theory,[9] the contribution to the proper self-energy from the exchange scattering process illustrated in Fig. 1(a) and Fig. 1(b) is given in Fig. 2(a). If we retain only this contribution, we are assuming the excited electron engages in spin-flip scattering from Stoner excitations. This is the scattering process invoked in various discussions of spin-dependent mean free paths in the literature. The analysis in Ref. 10 has this process in mind, for example, and the discussion there of the phenomenology of spin-dependent mean free paths is particularly complete.

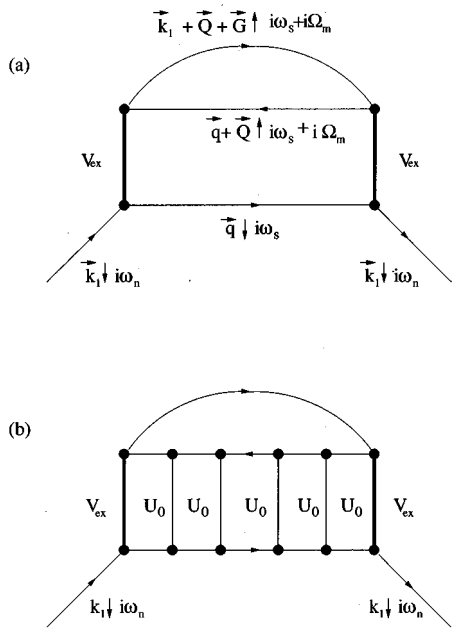

FIG. 2. (a) The contribution to self-energy of a spin-down electron, from the exchange scattering process illustrated in Fig. 1. The electron of wave vector $\vec{k}_1+\vec{Q}+\vec{G}$ is a plane-wave state, while the electrons of a wave vector $\vec{q}+\vec{Q}$ and $\vec{q}$ reside in the substrate energy bands. Here, $i\omega_s=2\pi(s+\frac{1}{2})/\beta$ and $i\Omega_m=2\pi m/\beta$ are the imaginary frequencies of many-body perturbation theory, where $\beta=1/(k_BT)$. (b) We include final-state interaction between the final-state electron and hole by summing the ladder graph series indicated.

Clearly, the scattering of the electron from spin waves, omitted from the picture just discussed, constitutes an additional mechanism for endowing the electron mean free path with a spin dependence. Consider, for example, an excited electron which propagates through a ferromagnet at absolute zero temperature. Then only spin-wave emission is possible. At zero temperature, it follows from angular momentum conservation that only excited electrons with spin down may emit spin waves. The reason is that when a spin wave is created, the z component of magnetization of the substrate is decreased by exactly the amount of $\hbar$.[11] This must be compensated by a change in angular momentum of the electron which has emitted the spin wave. If the excited electron has spin down, angular momentum will be conserved if its final state has spin up. If, however, the excited electron has spin up in the initial state, spin-wave emission is suppressed completely by considerations of angular momentum conservation.[12]

A central issue in the present paper is to asses the relative importance of spin-flip scattering from spin waves and that from Stoner excitations. From experimental data, one may infer that the inelastic mean-free paths of spin-down electrons is always shorter than that for spin-up electrons.[10] It is argued commonly, assuming that only the scattering process illustrated in Fig. 1(a) and Fig. 1(b) is operative, that this is so simply because there are more final states available to the spin-down electron, because there are more holes in the minority spin bands of the substrate.[10] Spin-wave emission provides a second mechanism for realizing shorter mean-free

path for spin-down electrons. If spin-wave emission is dominant, then the spin asymmetry in the mean free path has its origin in a very fundamental principle of physics, the conservation of angular momentum, rather than the details of the band structure. In this regard, we note that in a recent experimental study of an ultrathin Fe film, a strong signal from spin-wave scattering was reported in the SPEELS spectrum,[13] consistent with theoretical predictions.[7] Thus spin-wave scattering is surely present, in addition to that provided by Stoner excitations.

We may incorporate spin-wave emission into the analysis by going beyond the lowest contribution to the self-energy illustrated in Fig. 2(a). The collective excitations can be introduced by incorporating final-state interactions between the excited electron and hole, in the substrate energy bands.[14] The simplest scheme for doing this is illustrated in Fig. 2(b), where repeated scatterings of the electron and the hole are described by the ladder graph series depicted there. These graphs, applied to the analysis of the wave-vector- and frequency-dependent transverse susceptibility of the material, give a description of the spin waves and of the Stoner excitations as well.[7,14] In the present case, by virtue of the exchange matrix element through which the spin-triplet electron-hole pair in the substrate is excited, we shall encounter a response function distinctly different from the transverse spin susceptibility discussed commonly in the literature on itinerant ferromagnets.[14,15]

It is a straightforward exercise in diagrammatic perturbation theory to sum the diagrams illustrated in Fig. 2(b). As a consequence, we shall only state their contribution to the final form of the proper self-energy. We encounter three distinct response functions in the analysis. These have been discussed earlier.[7] We have, with $\vec{G}$ a reciprocal lattice vector,

$$\chi^{(0)}_{\downarrow\uparrow}(\vec{Q};\Omega)=\frac{1}{N}\sum_{\vec{q}}\frac{f(\epsilon_\uparrow(\vec{q}+\vec{Q}))-f(\epsilon_\downarrow(\vec{q}))}{\epsilon_\downarrow(\vec{q})-\epsilon_\uparrow(\vec{q}+\vec{Q})-\Omega-i\eta}, \quad (10)$$

$$\chi^{(1)}_{\downarrow\uparrow}(\vec{k}_1,\vec{Q},\vec{G};\Omega)=\sum_{\vec{q}}\tilde{V}_{ex}(\vec{k}_1,\vec{Q},\vec{q},\vec{G})\frac{f(\epsilon_\uparrow(\vec{q}+\vec{Q}))-f(\epsilon_\downarrow(\vec{q}))}{\epsilon_\downarrow(\vec{q})-\epsilon_\uparrow(\vec{q}+\vec{Q})-\Omega-i\eta}, \quad (11)$$

and also

$$\chi^{(2)}_{\downarrow\uparrow}(\vec{k}_1,\vec{Q},\vec{G};\Omega)=\sum_{\vec{q}}|\tilde{V}_{ex}(\vec{k}_1,\vec{Q},\vec{q},\vec{G})|^2\frac{f(\epsilon_\uparrow(\vec{q}+\vec{Q}))-f(\epsilon_\downarrow(\vec{q}))}{\epsilon_\downarrow(\vec{q})-\epsilon_\uparrow(\vec{q}+\vec{Q})-\Omega-i\eta}, \quad (12)$$

where we have

$$\tilde{V}_{ex}(\vec{k}_1,\vec{Q},\vec{q},\vec{G})=\frac{1}{V_c}\sum_{\vec{G}'}V(\vec{k}_1-\vec{q}+\vec{G}')\times f(\vec{q}+\vec{Q}-\vec{G}'+\vec{G})f(\vec{q}-\vec{G}'). \quad (13)$$

The diagrams in Fig. 2(b) give

$$\Sigma_\downarrow(\vec{k}_1,E+i\eta)=\frac{1}{\pi}\sum_{\vec{G}}\sum_{\vec{Q}}\int_{-\infty}^{\infty}d\Omega\frac{1+n(\Omega)}{E+i\eta-\Omega-\epsilon_\uparrow(\vec{k}_1+\vec{Q}+\vec{G})}\times\mathrm{Im}\left[\chi^{(2)}_{\downarrow\uparrow}(\vec{k}_1,\vec{Q},\vec{G};\Omega)+\frac{U_0}{N}\frac{[\chi^{(1)}_{\downarrow\uparrow}(\vec{k}_1,\vec{Q},\vec{G};\Omega)]^2}{1-U_0\chi^{(0)}_{\downarrow\uparrow}(\vec{Q};\Omega)}\right]. \quad (14)$$

Here, $n(\Omega)=[\exp(\hbar\Omega/k_BT)\text{-}1]^{-1}$ is the Bose-Einstein function. Note that the exchange matrix element scales as $1/N$, the number of unit cells in the crystal. Then, of course, the self-energy is independent of N as it must be. In these expressions $\epsilon_{\uparrow,\downarrow}(\vec{k})=\epsilon_0(\vec{k})+U_0n_{\downarrow,\uparrow}$, where n_σ is the number of electrons with spin σ in each unit cell, and $\epsilon_0(\vec{k})$ describes the energy band in the paramagnetic state.

If we retain only the contribution from $\chi^{(2)}_{\downarrow\uparrow}$ in Eq. (14), then we have a description of scattering of the excited electron from only Stoner excitations, as illustrated in Fig. 2(a). The spin-wave emission process enters through the term proportional to $(\chi^{(1)}_{\downarrow\uparrow})^2$; the spin waves produce poles in this contribution, generated by the zeros of the denominator.

In a similar manner, one can generate an expression for the proper self-energy of a spin-up electron, We find

$$\Sigma_\uparrow(\vec{k}_1,E+i\eta)=\frac{1}{\pi}\sum_{\vec{G}}\sum_{\vec{Q}}\int_{-\infty}^{\infty}d\Omega\frac{1+n(\Omega)}{E+i\eta-\Omega-\epsilon_\downarrow(\vec{k}_1+\vec{Q}+\vec{G})}+\mathrm{Im}\left[\chi^{(2)}_{\uparrow\downarrow}(\vec{k}_1,\vec{Q},\vec{G};\Omega)+\frac{U_0}{N}\frac{[\chi^{(1)}_{\uparrow\downarrow}(\vec{k}_1,\vec{Q},\vec{G};\Omega)]^2}{1-U_0\chi^{(0)}_{\uparrow\downarrow}(\vec{Q};\Omega)}\right], \quad (15)$$

where

$$\chi^{(0)}_{\uparrow\downarrow}(\vec{Q};\Omega)=\frac{1}{N}\sum_{\vec{q}}\frac{f(\epsilon_\downarrow(\vec{q}+\vec{Q}))-f(\epsilon_\uparrow(\vec{q}))}{\epsilon_\uparrow(\vec{q})-\epsilon_\downarrow(\vec{q}+\vec{Q})-\Omega-i\eta}, \quad (16)$$

$$\chi^{(1)}_{\uparrow\downarrow}(\vec{k}_1,\vec{Q},\vec{G};\Omega)=\sum_{\vec{q}}\tilde{V}_{ex}(\vec{k}_1,\vec{Q},\vec{q},\vec{G})\frac{f(\epsilon_\downarrow(\vec{q}+\vec{Q}))-f(\epsilon_\uparrow(\vec{q}))}{\epsilon_\uparrow(\vec{q})-\epsilon_\downarrow(\vec{q}+\vec{Q})-\Omega-i\eta}, \quad (17)$$

$$\chi^{(2)}_{\uparrow\downarrow}(\vec{k}_1,\vec{Q},\vec{G};\Omega)=\sum_{\vec{q}}|\tilde{V}_{ex}(\vec{k}_1,\vec{Q},\vec{q},\vec{G})|^2\frac{f(\epsilon_\downarrow(\vec{q}+\vec{Q}))-f(\epsilon_\uparrow(\vec{q}))}{\epsilon_\uparrow(\vec{q})-\epsilon_\downarrow(\vec{q}+\vec{Q})-\Omega-i\eta}. \quad (18)$$

One identity is useful to note. We have

$$\chi^{(0)}_{\downarrow\uparrow}(\vec{Q},\Omega)=\chi^{(0)}_{\uparrow\downarrow}(\vec{Q},-\Omega)^*. \quad (19)$$

We comment on the manner in which the spin-wave contributions enter the expressions set down above. As noted earlier, in the spin-wave frequency domain, the function $1/[1\text{-}U_0\chi^{(0)}_{\downarrow\uparrow}(\vec{Q},\Omega)]$ has poles when $\Omega=\Omega(\vec{Q})$, where $\Omega(\vec{Q})$ is

the frequency of the spin wave of wave vector $\vec{Q}$. We shall be interested below in examining the contribution to the proper self-energy from the emission and absorption of long-wavelength spin excitations; so we isolate their contribution to the proper self-energy. Suppose we examine the limit $\vec{Q} \rightarrow 0$. Then after a bit of algebra, we find

$$\lim_{\vec{Q}\rightarrow 0} \frac{1}{1-U_0\chi^{(0)}_{\downarrow\uparrow}} = \frac{U_0\Delta n}{DQ^2-\Omega+i\eta}, \tag{20}$$

which shows that the spin-wave pole provides the dominant contribution to the term proportional to $[\chi^{(1)}_{\downarrow\uparrow}(\vec{k}_1,\vec{Q},\vec{G};\Omega)]^2$ in the proper self-energy. The spin-wave exchange stiffness D is given by[14]

$$D=\frac{1}{3\Delta n}\left\{\frac{1}{2N}\sum_{\vec{q}}\,[f(\epsilon_\uparrow(\vec{q}))+f(\epsilon_\downarrow(\vec{q}))]\nabla^2_{\vec{q}}\epsilon_0(\vec{q}) - \frac{1}{NU_0\Delta n}\sum_{\vec{q}}\,[f(\epsilon_\uparrow(\vec{q}))-f(\epsilon_\downarrow(\vec{q}))]|\nabla_{\vec{q}}\epsilon_0(\vec{q})|^2\right\}. \tag{21}$$

The contribution to the self-energy from scattering off long-wavelength spin waves is found by inserting Eq. (20) into Eqs. (14) and (15), after noting the identity in Eq. (19). We may set $\vec{Q}=0, \Omega=0$ in $\chi^{(1)}_{\uparrow\downarrow}(\vec{k}_1,\vec{Q},\vec{G};\Omega)$ and $\chi^{(1)}_{\downarrow\uparrow}(\vec{k}_1,\vec{Q},\vec{G};\Omega)$. Then we find

$$\Sigma_\downarrow(\vec{k}_1,E)=\frac{J^2(\vec{k}_1)}{N}\sum_{\vec{Q}}\frac{1+n(DQ^2)}{E-DQ^2-\epsilon_\uparrow(\vec{k}_1+\vec{Q})+i\eta} \tag{22}$$

and

$$\Sigma_\uparrow(\vec{k}_1,E)=\frac{J^2(\vec{k}_1)}{N}\sum_{\vec{Q}}\frac{n(DQ^2)}{E+DQ^2-\epsilon_\downarrow(\vec{k}_1+\vec{Q})+i\eta}. \tag{23}$$

Here $J(\vec{k}_1)$, which is the matrix element for emission or absorption of a long-wavelength spin wave by the electron, is given by

$$J^2(\vec{k}_1)=U_0^2\Delta n[\chi^{(1)}_{\downarrow\uparrow}(\vec{k}_1,0,0;0)]^2. \tag{24}$$

One sees easily that $\chi^{(1)}_{\downarrow\uparrow}(\vec{k}_1,0,0;0)=\chi^{(1)}_{\uparrow\downarrow}(\vec{k}_1,0,0;0)$. Note that we ignore umklapp scattering in this limiting form. For our model, we show the magnitude and energy variation of $J(\vec{k}_1)$ in Fig. 3.

The result in Eqs. (14) and (15), and also those just quoted, constitute the principal formal results on which our calculations are based. In Sec. III, we explore the contribution of long-wavelength spin waves to the self-energy, while in Sec. IV we discuss our numerical studies. The contribution to the mean free path of the scattering processes considered is found from the imaginary part of the self-energy as discussed below.

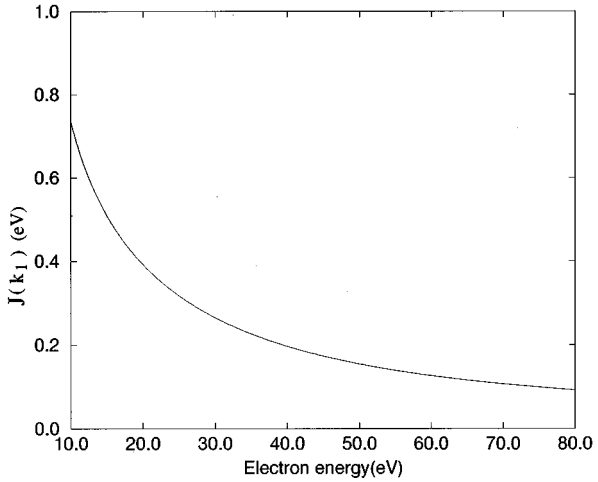

FIG. 3. The magnitude of the coupling constant $J(\vec{k}_1)$ for the emission and absorption of spin waves, as a function of electron energy. The analysis here determine only magnitude and not the sign of $J(\vec{k}_1)$.

III. REMARKS ON THE CONTRIBUTION TO THE QUASIPARTICLE LIFETIMES FROM THE EMISSION AND ABSORPTION OF LONG-WAVELENGTH SPIN WAVES

The primary objective of this paper is the evaluation of the contribution of the spin-flip scatterings to the lifetime of spin-up and spin-down quasiparticles, utilizing the expressions in Eqs. (14) and (15) for the basis of numerical calculations. For the ferromagnetic transition metals, we may expect finite-temperature effects to be small; so we proceed in our full calculations by setting the temperature $T=0$ everywhere. This is clearly a valid procedure for the Stoner excitations, since these have energies in the range of 0.5–3 eV, depending on the material of interest. Spin waves in the ferromagnetic transition metals are sufficiently ''stiff'' that even at room temperature, only rather long-wavelength modes are excited. Thus over most of the three-dimensional Brillouin zone, we may set the Bose-Einstein factor equal to zero. As an example, for Fe, $D\cong 300$ meV-A^2. If we estimate the wave vector of the thermally excited spin waves by setting DQ_T^2 equal to k_BT, then at room temperature $Q_T \cong 0.3A^{-1}$, a small fraction of the distance to the zone boundary; only a few percent of the Brillouin zone contains thermally excited spin waves. Thus, in fact, we may let $T\rightarrow 0$ when we examine the spin-wave contribution as well.

Nonetheless, despite these remarks, an interesting issue arises when we consider the contribution to the imaginary part of the proper self-energy from thermally excited spin waves, when $T\neq 0$. In this section, we explore this question.

In Eqs. (22) and (23), $\epsilon_{\uparrow,\downarrow}(\vec{k}_1+\vec{Q})$ enters through the propagator of the final-state electron. These energies in our model are given by $\{\hbar^2(\vec{k}_1+\vec{Q})^2/2m+V^{(1)}_{\uparrow,\downarrow}+iV^{(2)}_{\uparrow,\downarrow}\}$, where $V^{(1)}_{\uparrow,\downarrow}, V^{(2)}_{\uparrow,\downarrow}$ are real and imaginary parts of the proper self-energy of the final-state electron.

Suppose, for example, we consider the contribution to the imaginary part of the proper self-energy of spin-down electrons from emission of long-wavelength spin waves. In Eq. (22), we let E approach the real axis, to become

$\{\hbar^2(\vec{k}_1)^2/2m+V_\downarrow^{(1)}\}$. Thus we consider

$$\Sigma_\downarrow(\vec{k}_1,\epsilon_\downarrow(\vec{k}_1))=\frac{J^2(\vec{k}_1)}{N}\sum_{\vec{Q}}\frac{1+n(DQ^2)}{(\hbar^2/2m)[\vec{k}_1^2-(\vec{k}_1+\vec{Q})^2]-DQ^2+(V_\downarrow^{(1)}-V_\uparrow^{(1)})-iV_\uparrow^{(2)}}. \tag{25}$$

The long-wavelength spin waves have a very small energy; so the factor of DQ^2 may be ignored in the denominator of Eq. (25). It will be important to retain $\Delta V=V_\downarrow^{(1)}-V_\uparrow^{(1)}$, which we may suppose is positive. Note that $V_\uparrow^{(2)}=-\hbar/\tau_\uparrow$, where $\tau_\uparrow$ is the lifetime of the final-state, spin-up electron. When the sum on $\vec{Q}$ is converted to an integral, and once again we consider the contribution from long-wavelength modes, we have

$$\mathrm{Im}\{\Sigma_\downarrow(\vec{k}_1,\epsilon_\downarrow(\vec{k}_1))\}=\frac{J^2(\vec{k}_1)V_c}{8\pi^3}\int d^3Q[1+n(DQ^2)]\times\mathrm{Im}\left\{\frac{1}{\Delta V-\hbar\vec{v}_{\vec{k}_1}\cdot\vec{Q}+i\hbar/\tau_\uparrow}\right\}. \tag{26}$$

It is a straightforward matter to perform the integration over the direction of the spin wave vector $\vec{Q}$, to find

$$\mathrm{Im}\{\Sigma_\downarrow(\vec{k}_1,\epsilon_\downarrow(\vec{k}_1))\}=-\frac{J^2(\vec{k}_1)V_c}{4\pi^2\hbar v_{\vec{k}_1}}\int_0^\infty dQQ[1+n(DQ^2)]\times\tan^{-1}\left[\frac{2v_{\vec{k}_1}\hbar}{\tau_\uparrow}\frac{\hbar v_{\vec{k}_1}Q}{(\Delta V)^2+\left(\frac{\hbar}{\tau_\uparrow}\right)^2-(\hbar v_{\vec{k}_1}Q)^2}\right]. \tag{27}$$

The quantity $\mathrm{Im}\{\Sigma_\downarrow(\vec{k}_1,\epsilon_\downarrow(\vec{k}_1))\}$ is given by a virtually identical expression, except that $\tau_\uparrow$ is replaced by $\tau_\downarrow$, and also $[1+n(DQ^2)]$ becomes $n(DQ^2)$. Here $\vec{v}_{\vec{k}_1}=\hbar\vec{k}_1/m$ is the velocity of the electron of interest.

Our attention is directed toward the contribution proportional to the Bose-Einstein factor, $n(DQ^2)$. Note that as $Q\to 0$, $n(DQ^2)\to k_BT/DQ^2$; so the integral which involves this factor diverges logarithmically as $\vec{Q}\to 0$, if this and the phase space factor QdQ are all that is involved.

One may show very easily that if the self-energy corrections represented by ΔV and by $\tau_\uparrow$ are set aside by letting $\tau_\uparrow\to\infty$, and then by letting $\Delta V\to 0$, the logarithmic divergence survives . We may see this from Eq. (27) by first allowing $\tau_\uparrow\to\infty$. Then the $\tan^{-1}$ in this expression equals zero when $\hbar v_{\vec{k}_1}Q\leqslant\Delta V$, and switches to π when $\hbar v_{\vec{k}_1}Q\geqslant\Delta V$. There is thus a cutoff in the integral as $Q\to 0$, at $Q_c=\Delta V/\hbar v_{\vec{k}_1}$. Now if $\Delta V\to 0$, $Q_c\to 0$, and we realize the logarithmic divergence.

So if we consider an idealized excited electron with infinite lifetime propagating through our crystal, we set aside the dependence of its energy on spin direction provided by the inner potential; this electron may emit an infinite number of ''soft'' spin waves, if the crystal is at any finite temperature. The self-energy then diverges.

The dependence of the electron's energy on spin direction, as provided by the inner potential, blunts the divergence by introducing a cutoff wave vector Q_c. The divergence also is limited if the quasiparticle lifetime is finite.

For the purpose of illustration, we quote two limiting forms for $\mathrm{Im}\{\Sigma_\downarrow^{(T)}(\vec{k}_1,\epsilon_\downarrow(\vec{k}_1))\}$, and $\mathrm{Im}\{\Sigma_\uparrow^{(T)}(\vec{k}_1,\epsilon_\uparrow(\vec{k}_1))\}$, the contribution to the proper self-energy from thermally induced spin-wave absorption and emission processes. One has the following limits.

(a) Very-low-temperature limit. Here, $\tan^{-1}$ may be replaced by its form appropriate to the limit $\vec{Q}\to 0$. Then

$$\mathrm{Im}\{\Sigma_\downarrow^{(T)}(\vec{k}_1,\epsilon_\downarrow(\vec{k}_1))\}=\mathrm{Im}\{\Sigma_\uparrow^{(T)}(\vec{k}_1,\epsilon_\uparrow(\vec{k}_1))\}=-\frac{J^2(\vec{k}_1)\hbar V_c}{4\pi^2\tau_{\uparrow,\downarrow}}\frac{\zeta_{3/2}(1)}{(\Delta V)^2+\left(\hbar/\tau_{\uparrow,\downarrow}\right)^2}\times\left(\frac{k_BT}{D}\right)^{3/2}, \tag{28}$$

where $\zeta_{3/2}(1)$ is the zeta function with argument unity. Here the scattering rate in the end scales simply as the number of thermally excited spin waves, which for the ferromagnet scales as $T^{3/2}$.

(b) The limit $\hbar/\tau_{\uparrow,\downarrow}\ll\Delta V$. Here $\tan^{-1}$ maybe replaced by zero when $Q\leqslant Q_c$, and π when $Q\geqslant Q_c$. We then find

$$\mathrm{Im}\{\Sigma_\downarrow^{(T)}(\vec{k}_1,\epsilon_\downarrow(\vec{k}_1))\}=\mathrm{Im}\{\Sigma_\uparrow^{(T)}(\vec{k}_1,\epsilon_\uparrow(\vec{k}_1))\}=-\frac{J^2(\vec{k}_1)V_c}{8\pi\hbar v_{\vec{k}_1}}\frac{k_BT}{D}\left\{\ln\left(\frac{1}{1-e^{-DQ_c^2/k_BT}}\right)\right\}. \tag{29}$$

When scatterings of excited electrons are discussed, distinctly different lifetimes enter, depending on the physical phenomenon of interest. In this paper we examine only the *quasiparticle* lifetime, which is the probability an electron in a particular state $\vec{k}_1$ remains in that state, after time t. We have seen that at finite temperature, the contribution to the decay rate of this state is influenced sensitively by the self-energy of the electrons involved in the spin-wave absorption or emission process. The quasiparticle lifetime controls photoemission intensities, the probing depth of the secondary electron microscopy, and related issues.

The *transport* lifetime of quasiparticles near the Fermi surface controls the electrical resistivity, and is of a fundamentally different nature. Here we have an electric current,

and this lifetime describes the decay of that current. It is thus the change in electron momentum parallel to the current direction that enters; there is, in the final expression, a factor of $(1-\cos\theta)$ absent in the quasiparticle lifetime, where θ is the angle between the incident and final-state electron momentum. In a spin-wave emission or absorption process, as $Q \rightarrow 0$, one encounters an additional factor of Q^2 in the transport lifetime that suppresses the infrared ''near divergence'' present in the quasiparticle lifetime.

We now turn to our numerical studies at $T=0$, since we see that the finite temperature correction are modest, once it is recognized the ''near divergence'' is suppressed, for the reasons just discussed.

IV. NUMERICAL STUDIES OF THE SPIN-FLIP CONTRIBUTION TO THE PROPER SELF-ENERGY AT $T=0$

In this section, we present our numerical studies of the contribution to the imaginary part of the self-energy, from the spin-flip exchange scattering discussed above. While our model clearly contains oversimplifications if we have applications to real materials in mind, as mentioned above it is our view that with the appropriate choice of parameters, we can simulate the trends found in real $3d$ transition ferromagnets, and obtain results which can be set alongside data. Note, for example, that the authors of Ref. 10 argue that the spin-dependent portion of the electron mean-free path is influenced only by the relative number of majority and minority spin holes found in the d bands. If we accept this view for the moment, then we may suppose that the actual details of the band structure, crystal structure, etc., are of secondary importance. We proceed within the framework of this philosophy for the purpose of the present paper.

We begin by choosing the value of the nearest-neighbor hopping integral so that the width of the substrate energy band is 4 eV, a value close to that of the ferromagnetic $3d$ transition metals Fe, Co, and Ni. We must then choose values for the Fermi energy E_F and the Coulomb interaction strength U_0. For this purpose, we employ the information in Table 1 in Ref. 10. For Fe, Co, and Ni, these authors give values for $n=(n_\uparrow+n_\downarrow)/2$ and $\Delta n=(n_\uparrow-n_\downarrow)/(n_\uparrow+n_\downarrow)$. We choose values for E_F and U_0, to match these numbers as well as we can, and maintain a ferromagnetic state in our model. Of course, we have only a single band of electrons in our model substrate; so we must divide the numbers in Ref. 10 by 5. For Co, we can match the numbers well with $n=0.825$ and $\Delta n=0.175$ in our model, compared to 0.825 and 0.17 in Table 1 of Ref. 10. For our simulation of Fe, we have $n=0.8$ and $\Delta n=0.2$, compared to 0.7 and 0.22 for actual Fe. Finally, for Ni, we have in our model $n=0.9$ and $\Delta n=0.1$, compared to $n=0.95$ and $\Delta n=0.05$. As we can see, in the case of Ni, with our model we cannot reproduce both the correct values of n and Δn. Values for U_0 required to achieve these number range from 5 eV to 8 eV. We should refer to our three cases pseudo Fe, pseudo Co, and pseudo Ni, respectively.

With the model parameters chosen as just discussed, in Fig. 4 we show the imaginary part of proper self-energy, for spin-up and -down electrons, for our pseudo Fe. In this figure, the zero of energy is chosen as the Fermi energy. The

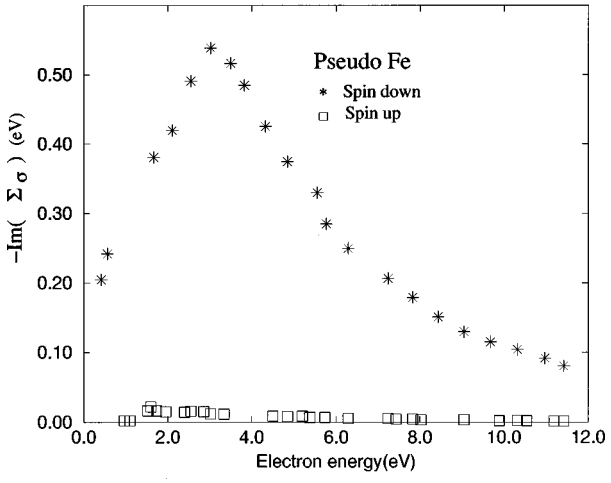

FIG. 4. The imaginary part of contribution to the proper self-energy from exchange scattering, as a function of electron energy. The calculation is for zero temperature. The stars provide the quantity for spin-down electrons and the squares for spin-up electrons. Electron energy is measured from the Fermi surface. The results are for our model description of Fe.

calculations are for the absolute zero of temperature. At $T=0$, the imaginary part of the self-energy must vanish at the Fermi energy. Careful examination of the self-energy near the Fermi energy shows that indeed it vanishes as E_F is approached. This cannot be appreciated from the energy scale used in Fig. 4.

The imaginary part of the self-energy we calculate here is related to the quasiparticle lifetime τ_σ of an electron of spin σ as follows. Both spin-flip (SF) and non-spin-flip (NSF) scatterings contribute to limiting its lifetime. These are additive if we consider the inverse of the lifetime or, equivalently, the scattering rate. Thus, we may write

$$\frac{1}{\tau_\sigma}=\left(\frac{1}{\tau_\sigma}\right)_{NSF}+\left(\frac{1}{\tau_\sigma}\right)_{SF}. \tag{30}$$

We have

$$\left(\frac{1}{\tau_\sigma}\right)_{SF}=-\frac{1}{\hbar}\mathrm{Im}(\Sigma_\sigma) \tag{31}$$

where $-\mathrm{Im}(\Sigma_\sigma)$ is illustrated in Fig. 4 and the subsequent figure.

We comment on two features evident in the results presented in Fig. 4. First, a spin-up quasiparticle engages in very few exchange-induced spin-flip scatterings. We have

$$\left(\frac{1}{\tau_\downarrow}\right)_{SF}\gg\left(\frac{1}{\tau_\uparrow}\right)_{SF} \tag{32}$$

for all energies shown in this figure. The contrast between the two is more than one order of magnitude. We have found this to be the case in all the calculations we have performed for our model materials. Thus, in what follows, we concentrate only on $\mathrm{Im}(\Sigma_\downarrow)$, and ignore the influence of $\mathrm{Im}(\Sigma_\uparrow)$.

We also see that for energies close to the Fermi energy, $-\mathrm{Im}(\Sigma_\downarrow)$ increases with electron energy, to peak at roughly 4 eV above, and then falls off with increasing energy. The

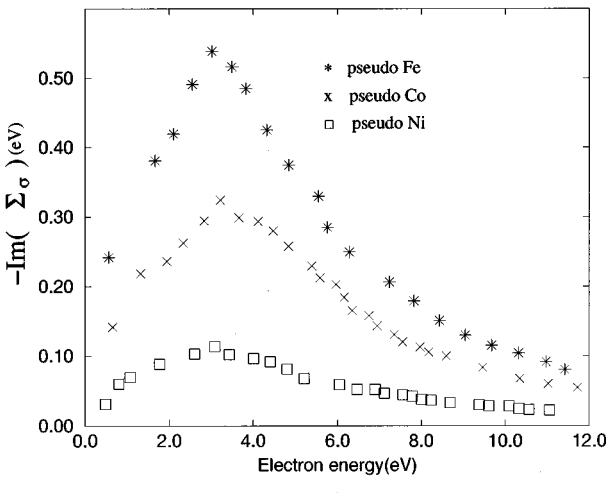

FIG. 5. A comparison of the imaginary part of the spin-flip contribution to the proper self-energy of spin-down excited electrons for our model descriptions of the three transition metal ferromagnets.

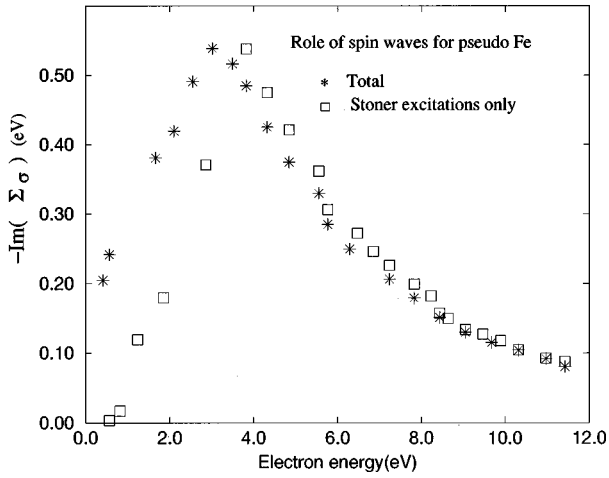

FIG. 6. For our model of Fe, we show the spin-flip inelastic scattering to the imaginary part of the proper self-energy of excited electrons in Fe for two pictures. In one, only the scattering from Stoner excitations is included (squares), and in the second, that from both Stoner excitations and spin waves is included (asterisks).

data reported in Ref. 5, which probes the energy variation of the quasiparticle lifetime for excitations within an electron volt of the Fermi energy of Co is compatible with these results and those presented below. That is, these authors measure a scattering rate which increases, with increasing quasiparticle energy, in the range they explored. For the $3d$ transition metal ferromagnets, work functions are roughly 4.5 eV. Thus, photoelectron spectroscopies and also other probes of the surface with electron beams employ an electron whose energy lies above the maximum in Fig. 4. Thus, one has for such studies a spin-flip scattering rate which falls off with increasing electron energy, from Fig. 4.

In Fig. 5, we present calculations of the rate for spin-flip processes for our three model ferromagnetic metals. For all energies, we see that the spin-flip scattering rate falls off as we move from Fe, to Co, and then to Ni. This behavior is, in a qualitative sense, compatible with the empirically based arguments presented in Ref. 10. These authors argue the scattering rate from the exchange process for spin-down electrons should scale linearly with the number of minority spin holes in the d band. For our pseudo Fe, Co, and Ni, we have 0.4, 0.35, and 0.2 holes, respectively. At all energies, in Fig. 5 we see that $-\mathrm{Im}(\Sigma_{\downarrow})$ indeed falls off with decreasing number of minority spin holes. However, the scaling is qualitative, rather than quantitative. We would expect, if only the number of holes mattered, that the scattering rate for pseudo Co would differ from that for pseudo Fe by roughly 12%. We see a large difference. This is true also for Ni, where our calculated differences are considerably larger than the factor of 2 expected from the empirical rule set forth in Ref. 10.

As noted above, for our three simulated metals, we find $-\mathrm{Im}(\Sigma_{\uparrow})$ to be very small always. This should scale, according to the arguments in Ref. 10, as the number of majority spin holes in the d band. For all three of our models, the majority spin band is very nearly filled. We would thus expect $-\mathrm{Im}(\Sigma_{\uparrow})$ to be very small according to this rule, but we cannot test it. We thus moved the Fermi level to achieve a model ferromagnet with 0.164 minority spin holes and 0.06 majority spin holes. We find $\mathrm{Im}(\Sigma_{\uparrow})$ much larger for this case. However, the ratio of $\mathrm{Im}(\Sigma_{\uparrow})/\mathrm{Im}(\Sigma_{\uparrow})$ is in the range of 4.5 for the energies we explored, considerably larger than the factor of 2.9 expected from the arguments in Ref. 10.

Thus, we conclude that it is indeed the case, for the calculations we have carried out, that $\mathrm{Im}(\Sigma_{\sigma})$ has a magnitude which varies monotonically with the number of holes in the relevant substrate d band. However, the variation is clearly stronger than the simple linear relationship suggested in Ref. 10. This rule thus does not serve as a guide at the quantitative level to judge from our model study.

A final question we examine is the role of spin-wave scattering, compared to that from Stoner excitations. We have explored this as follows. If we retain in Eq. (14) only the term $\chi^{(2)}_{\downarrow\uparrow}$ on the right hand side, then we have in the analysis only scattering from Stoner excitations. Inclusion of inelastic scattering from spin waves requires one to retain the term proportional to $(\chi^{(1)}_{\downarrow\uparrow})^2$; as noted above, the spin waves enter through poles in the function $[1-U_0\chi_{\downarrow\uparrow}]^{-1}$. By comparing the complete calculation discussed above with those based on retaining only $\chi^{(2)}_{\downarrow\uparrow}$, we may assess the role of spin-wave scattering.

We show such a comparison in Fig. 6 for pseudo Fe. Above the peak in the imaginary part of the proper self-energy, we see little difference between the two results. Thus, at these higher energies, spin waves play a modest role, and the dominant scattering is from the Stoner excitations. However, as we drop below the peak, we see a dramatic difference between the two results. The scattering rate calculated upon including only Stoner excitations falls far below that of the full calculation, with spin waves included. Clearly, spin-wave scattering is dominant at low energies. We have found very similar results for our pseudo Co and pseudo Ni. This suggests that the experiments in Ref. 5 explore the regime where spin-wave scattering dominates.

V. RESULTS AND DISCUSSIONS

In this paper, we have presented a series of studies of the spin-flip inelastic exchange scattering of excited electrons

from the spin excitations of model itinerant electron ferromagnets. While our picture of the electronic structure of the substrate is a rather simple one, we have seen that the calculations account nicely for general trends seen in the experimental data, and also allow us to explore the dependence of the scattering rate on the number of holes in the relevant energy bands. Spin-wave scattering is seen to be a dominant source of inelastic scattering for electrons whose energy lies below 3 eV or so from the Fermi energy. At higher energies, above the peak in the imaginary part of the self-energy, scattering from Stoner excitations is dominant.

We conclude with remarks on an issue addressed in Sec. I, now that our results have been discussed. Pappas and coworkers measured a spin asymmetry in the electron transmission through ultrathin films of Fe deposited on Cu(100), and argued that the spin asymmetry in the inelastic mean free path is responsible for the fact that majority spin electrons have higher transmissivity than minority spin electrons.[2] Our calculations indeed show a very strong spin dependence in $\mathrm{Im}(\Sigma_\sigma)$ for our model Fe, consistent with their proposal. However, shortly after their paper was published, Gokhale and Mills[3] reported calculations which illustrated that spin-dependent elastic scatterings alone account very nicely for spin asymmetries found in the transmissivity. We conclude by inquiring if the *inelastic* scattering rates calculated here are sufficiently strong to account for the data.

Of interest are electron kinetic energies 5–10 eV above the vacuum level. If we assume the inner potential is in the range of 10 eV, then we should use results such as those presented in Fig. 4 for kinetic energies in the 15–20 eV range. The velocity of such an electron is in the range of 3×10^8 cm/sec. In the energy regime of interest, from Fig. 4, our model of Fe gives $-\mathrm{Im}(\Sigma_\downarrow)\cong 0.1$ eV, and as we have seen, to an excellent approximation majority spin electrons suffer little spin-flip scattering. One may argue, possibly naively, that in real Fe, $-\mathrm{Im}(\Sigma_\downarrow)$ may be larger by a factor of 5 in this energy regime, since there are five *d* bands for each spin direction in Fe, and an excited electron in the energy range of interest can access the complete spectrum of Stoner excitations. This would imply the distance of travel between spin-flip events, $v(\tau_\downarrow)_{sf}$, is in the range of 40 Å. This suggests, consistent with the arguments put forth in Ref. 3, that the spin-flip inelastic scattering rate is too weak to account for the rather large transmission asymmetry reported by Pappas *et al.*, in the energy range explored by them.

Calculations based on a realistic electronic structure for Fe will be required, of course, for this conclusion to be put on a firm footing, but the results here are suggestive, in our mind. We note with interest a recent experiment in which both the elastic and inelastic contributions to the transmissivity of electrons through ultrathin film of Co have been determined separately.[16] The analysis concludes that elastic scatterings are indeed the dominant source of the total spin asymmetry in the transmission coefficient.

ACKNOWLEDGMENT

This research has been supported by the U.S. Department of Energy, through Grant No. DE-FG03-84ER 45083.

[1] *Polarized Electrons in Surface Physics*, edited by R. Feder (World Scientific, Singapore, 1985).
[2] D. P. Pappas, K. P. Kämper, B. P. Miller, H. Hopster, D. E. Fowler, C. R. Brundle, A. C. Luntz, and Z. X. Shen, Phys. Rev. Lett. **66**, 504 (1991).
[3] M. P. Gokhale and D. L. Mills, Phys. Rev. Lett. **66**, 2251 (1991).
[4] A. Ormeci, B. M. Hall, and D. L. Mills, Phys. Rev. B **42**, 4524 (1991).
[5] M. Aeschlimann, M. Bauer, S. Pawlik, W. Weber, R. Burgermeister, D. Oberil, and H. C. Siegmann, Phys. Rev. Lett. **79**, 5158 (1997).
[6] J. B. Pendry, *Low Energy Electron Diffraction* (Academic Press, London, 1974); also M. A. Van Hove and S. Y. Tong, *Surface Crystallography by LEED* (Springer-Verlag, Heidelberg, 1979).
[7] M. Plihal and D. L. Mills, Phys. Rev. B **58**, 14 407 (1998).
[8] W. E. Pickett, S. C. Ewrin, and E. C. Ethridge, Phys. Rev. B **58**, 1201 (1998).
[9] See, for example, A. A. Abrikosov, L. P. Gorkov, and I. E. Dzyaloshinski, *Methods of Quantum Field Theory in Statistical Physics* (Prentice-Hall, Englewood Cliffs, NJ, 1963).
[10] G. Schönhense and H. C. Siegmann, Ann. Phys. (Leipzig) **2**, 465 (1993).
[11] C. Kittel, *Quantum Theory of Solids* (Wiley, New York, 1963), Chap. 4.
[12] In these remarks, we assume that spin orbit coupling is weak and may be ignored.
[13] M. Plihal, D. L. Mills, and J. Kirschner, Phys. Rev. Lett. **82**, 2579 (1999).
[14] T. Izuyama, D. J. Kim, and R. Kubo, J. Phys. Soc. Jpn. **18**, 1025 (1963).
[15] H. Tang, M. Plihal, and D. L. Mills, J. Magn. Magn. Mater. **187**, 23 (1998).
[16] D. Oberli, R. Burgermeister, S. Riesen, W. Weber, and H. C. Siegmann, Phys. Rev. Lett. **81**, 4228 (1998).